



Excitation of a Gould-Trivelpiece (TG) Mode by Relativistic Electron Beam (REB) in Magnetized Dusty Plasma

Research Article

D. Kaur¹, Suresh C. Sharma^{2,*} and R.S. Pandey¹

¹Amity Institute of Applied Sciences, Amity University, Sector 125, Noida 201313, Uttar Pradesh, India

²Department of Applied Physics, Delhi Technological University, Bawana Road, Delhi 110042, India

*Corresponding author: suresh321sharma@gmail.com

Abstract. Gould-Trivelpiece (TG) mode is excited by a relativistic electron beam (REB) via Cerenkov interaction in a magnetized dusty plasma and dusty plasma cylinder. The unstable wave's frequency increases with relative density of negatively charged dust grains $\delta (= n_{i0}/n_{e0})$, where n_{i0} is the equilibrium ion density, n_{e0} is the equilibrium electron density, respectively) in both infinite and finite geometry. The growth rate of the unstable mode increases with beam density and scales as one third power of beam density in both the cases. In addition, the growth rate of the unstable mode decreases with relativistic gamma factor. Moreover, comparison between the infinite and finite geometry indicates that the unstable mode's growth rate is more in case of infinite geometry than that of the finite geometry. Our theoretical results are in line with some of the experimental observations and theoretical findings of previous investigations.

Keywords. Relativistic electron beam; Dust grains; Growth rate; Finite geometry; Infinite geometry

PACS. 51.60.+a

Received: May 26, 2018

Accepted: June 14, 2018

Copyright © 2018 D. Kaur, Suresh C. Sharma and R.S. Pandey. This is an open access article distributed under the Creative Commons Attribution License, which permits unrestricted use, distribution, and reproduction in any medium, provided the original work is properly cited.

1. Introduction

Gould-Trivelpiece (TG) waves are electrostatic waves and considerably observed in the range of frequency between ion plasma frequency and electron cyclotron frequency. TG waves are also known by the name of *lower hybrid waves* (LHWs). These waves have been investigated by

many researchers both theoretically and experimentally [1–5] for many decades due to their property of absorbing and heating the electrons effortlessly near the boundary of the plasma. In bounded plasmas the TG wave appears as a short radial wavelength, whereas in unbounded plasmas it is linked with a short azimuthal wavelength [6].

Praburam and Sharma [7] have reported that low-energy beam of electrons excite the TG wave of higher harmonics. Seiler *et al.* [8] have used linear Princeton Q-1 device to investigate the instability of LHWs by a spiralling ion beam. The behaviour of LHW instability due to perpendicular ion beam has been observed by Chang [9]. The excitation of lower hybrid waves by a density modulated electron beam in a plasma cylinder has been studied by Sharma *et al.* [10]. Prakash *et al.* [11] have investigated the excitation of lower hybrid waves by an ion beam. They observed that LHW shows maximum growth rate of the instability when phase velocity of LHW along the magnetic field is similar to the electron thermal velocity.

Recently, a lot of work has been done by the researchers in plasma containing dust grains [12–17]. In laboratory, study has been conducted on the waves in non-magnetized [12] and weakly magnetized [13] dusty plasmas. Sharma *et al.* [14] have developed a model in which *ion-acoustic wave* (IAWs) have been excited by an ion beam in a magnetized dusty plasma cylinder. The behaviour of *dust-acoustic waves* (DAWs) instability due to an ion beam in infinite geometry dusty plasma has been studied by Sharma *et al.* [15]. In their study, they found that frequencies and the growth rate associated with DAWs instability increases with relative density of negatively charged dust grains.

Barkan *et al.* [16] have studied ion-acoustic waves in magnetized dusty plasma and found that the phase velocity of waves upraise with an increase in number density of negatively charged dust grains. A drastic reduction in the strength of the Landau damping has also been observed by them. Using Vlasov theory, Rosenberg [17] has studied instabilities of dust-ion acoustic mode as well as dust-acoustic modes in unmagnetized dusty plasma.

In the present work, a model is developed for excitation of *Gould-Trivelpiece* (TG) mode by a relativistic electron beam in a magnetized dusty plasma (infinite geometry) and magnetized dusty plasma cylinder (finite geometry). The instability analysis for infinite as well as finite geometries is given in Section 2. We have obtained the response of beam electrons, plasma electrons and plasma ions using fluid treatment. To derive the expressions for the instability growth rates in both the cases, we have used first order perturbation theory, and are mentioned in Section 3. Lastly, conclusion of the work is given in Section 4.

2. Instability Analysis

2.1 Infinite Geometry

We consider a plasma containing uniform dust grains having equilibrium electron density n_{e0} , ion density n_{i0} , and dust grain density n_{d0} . A static magnetic field B_s is applied in the z -direction. The charge, mass and temperature of plasma constituents are defined by $(-e, m_e, T_e)$

for electrons, (e, m_i, T_i) for ions and $(-Q_{d0}, m_d, T_d)$ for dust grains. Consider an electrostatic wave, say, *Gould-Trivelpiece* (TG) wave, propagating at an angle to the external magnetic field, with propagation vector k in the x-z plane. A *relativistic electron beam* (REB) propagates along the z-axis parallel to the magnetic field with uniform density n_{b0} and equilibrium velocity $v_{b0}\hat{z}$. The beam and plasma system prior to the perturbation is quasineutral, such that $(-n_{e0} + n_{i0} - n_{b0} - n_{d0} \simeq 0)$. This equilibrium is disturbed by an electrostatic perturbation and associated potential with it is given by

$$\Phi = \Phi_0 e^{[-i(\omega t - k_x x - k_z z)]} . \quad (1)$$

The dusty plasma species are taken as fluids and follow the equation of motion and continuity, given as

$$m_e \left[\frac{\partial \vec{v}}{\partial t} + (\vec{v} \cdot \nabla) \vec{v} \right] = -e\vec{E} - \frac{e}{c} \vec{v} \times \vec{B}_s, \quad (2)$$

$$\frac{\partial n}{\partial t} + \nabla \cdot (n\vec{v}) = 0. \quad (3)$$

Further, on linearization the equations of motion and continuity (cf. Eqs. (2) and (3)) lead to the electron density, ion density, dust density perturbations as:

$$n_{1e} = -\frac{n_{e0}e\Phi}{m_e} \left[\frac{k_x^2}{\omega^2 - \omega_{ce}^2} + \frac{k_z^2}{\omega^2} \right], \quad (4)$$

where $\omega_{ce} (= \frac{eB_s}{m_e c})$ is the electron-cyclotron frequency,

$$n_{1i} = \frac{n_{i0}e\Phi}{m_i} \left[\frac{k_x^2}{\omega^2 - \omega_{ci}^2} + \frac{k_z^2}{\omega^2} \right], \quad (5)$$

where $\omega_{ci} (= \frac{eB_s}{m_i c})$ is the ion-cyclotron frequency,

$$n_{1d} = -\frac{n_{d0}Q_{d0}\Phi k^2}{m_d \omega^2}. \quad (6)$$

The perturbed density of electrons of beam can be acquired by solving the relativistic equation of motion [18] and continuity (cf. Eq. (3)), we obtain

$$\frac{\partial(\gamma\vec{v})}{\partial t} + (\vec{v} \cdot \nabla)(\gamma\vec{v}) = -\frac{e\vec{E}}{m_0}, \quad (7)$$

$$\vec{v} = v_{b0}\hat{z} + \vec{v}_1, \quad \gamma\vec{v} = \gamma_0^3\vec{v}_1,$$

$$n_{1b} = \frac{-n_{b0}ek_z^2\Phi}{m_0\gamma_0^3(\omega - k_z v_{b0})^2}, \quad (8)$$

where $\gamma_0 = (1 - \frac{v^2}{c^2})^{-1/2}$ is the relativistic gamma factor, m_0 is the rest mass of electron. Here we have considered unmagnetized electron beam. In this case, dust is taken as unmagnetized since $\omega \gg \omega_{cd}$, where $\omega_{cd} (= \frac{Q_{d0}B_s}{m_d c})$ is the dust cyclotron frequency. Further applying the probe theory to dust particles, Q_d (dust grain's charge) is said to be well-adjusted with the plasma currents present on the grain surface as

$$-\frac{dQ_d}{dt} = I_e + I_i. \quad (9)$$

Following refs. [19,20], the dust grain surface will have electron and ion currents, and can be expressed as

$$I_e = -\pi\alpha^2 e \left(\frac{8T_e}{\pi m_e} \right)^{1/2} n_e \exp\left(\frac{e(\Phi_{g0} - V_1)}{T_e} \right),$$

$$I_i = \pi\alpha^2 e \left(\frac{8T_i}{\pi m_i} \right)^{1/2} n_i \left(1 - \frac{e(\Phi_{g0} - V_1)}{T_i} \right).$$

Here, the radius of the dust grain sphere is α , $(\Phi_{g0} - V_1)$ is the difference between the surface potential of the dust particles and plasma potential. In the absence of dust grains the electron density is n_e and ion density is n_i . If $|I_{e0}|$ and $|I_{i0}|$ are the equilibrium currents due to electron and ion on the grain surface, then, in equilibrium, $|I_{e0}| = |I_{i0}|$. As there is no plasma potential in equilibrium, therefore, $|I_{e0}|$ can be written as $|I_{e0}| = \pi\alpha^2 e \left(\frac{8T_e}{\pi m_e} \right)^{1/2} n_{e0} e^{(e\Phi_{g0}/T_e)}$. The dust charge fluctuation equation is expressed as

$$\frac{dQ_{1d}}{dt} + \eta Q_{1d} = -|I_{e0}| \left(\frac{n_{1i}}{n_{i0}} - \frac{n_{1e}}{n_{e0}} \right), \quad (10)$$

where $\eta = \left(\frac{|I_{e0}|e}{C_g} \right) \left(\frac{1}{T_e} + \frac{1}{T_i - e\Phi_{g0}} \right)$ is the dust charging rate and Q_{1d} is the perturbed dust grain charge and is given as $Q_{1d} = Q_d + Q_{d0}$. The capacitance of dust grain is denoted by $C_g = (a + a^2 \lambda_{De}^{-1})$ the electron Debye length. Replacing $\frac{d}{dt}$ by $-i\omega$ in Eq. (9), we and λ_{De} is deduce the dust grain charge fluctuation

$$Q_{1d} = \frac{|I_{e0}|}{i(\omega + i\eta)} \left(\frac{n_{1i}}{n_{i0}} - \frac{n_{1e}}{n_{e0}} \right). \quad (11)$$

Putting the values of n_{1e} and n_{1i} from Eqs. (4) and (5) in Eq. (11), we obtain

$$Q_{1d} = \frac{|I_{e0}|}{i(\omega + i\eta)} \left[\frac{k_x^2 \Phi}{(\omega^2 - \omega_{ci}^2) m_i} + \frac{k_z^2 \Phi}{m_i \omega^2} + \frac{k_x^2 \Phi}{m_e (\omega^2 - \omega_{ce}^2)} + \frac{k_z^2 \Phi}{m_e \omega^2} \right]. \quad (12)$$

Under the view of overall charge neutrality in equilibrium, we can write, $-en_{i0} + en_{e0} + Q_{d0}n_{d0} + en_{b0} = 0$ or $n_{d0}/n_{e0} = \{(\delta - 1) - n_{b0}/n_{e0}\} (e/Q_{d0})$, where $\delta = n_{i0}/n_{e0}$.

Using Poisson's equation $\nabla^2 \Phi = 4\pi(n_{1e}e - n_{1i}e + n_{1b}e + n_{d0}Q_{1d} + Q_{d0}n_{1d})$ and substituting the values from Eqs. (4)-(6), (8) and (12) in it, and taking $\omega \ll \omega_{ce}$, we obtain

$$1 + \left(\frac{\omega_{pe}^2 k_x^2}{\omega_{ce}^2 k^2} - \frac{\omega_{pe}^2 k_z^2}{\omega^2 k^2} - \frac{\omega_{pi}^2 k_x^2}{(\omega^2 - \omega_{ci}^2) k^2} \right) - \left(\frac{i\beta\omega_{pe}^2 (m_e/m_i) k_x^2}{(\omega + i\eta)(\omega^2 - \omega_{ci}^2) k^2} + \frac{i\beta\omega_{pe}^2 (m_e/m_i) k_z^2}{(\omega + i\eta)\omega^2 k^2} \right) + \left(\frac{i\beta\omega_{pe}^2 k_x^2}{(\omega + i\eta)\omega_{ce}^2 k^2} - \frac{i\beta\omega_{pe}^2 k_z^2}{(\omega + i\eta)\omega^2 k^2} + \frac{i\beta\omega_{pe}^2 k_z^2 \omega_{pd}^2}{(\omega + i\eta)\omega^2 k^2 \omega^2} \right) = \frac{\omega_{pb}^2 k_z^2}{\gamma_0^3 (\omega - k_z v_{b0})^2 k^2} \quad (13)$$

where $\omega_{pe}^2 = \frac{4\pi n_{e0} e^2}{m_e}$, $\omega_{pi}^2 = \frac{4\pi n_{i0} e^2}{m_i}$, $\omega_{pd}^2 = \frac{4\pi n_{d0} e^2}{m_d}$, $\omega_{pb}^2 = \frac{4\pi n_{b0} e^2}{m_0}$ and $\beta \left(= \frac{|I_{e0}| n_{d0}}{e n_{e0}} \right)$ is the dust plasma coupling parameter.

Using charge neutrality condition mentioned by Prakash and Sharma [21], we can also write dust plasma coupling parameter as $\beta = 0.1\pi\alpha^2 n_{d0} v_{te}$, where $v_{te} \left(= \sqrt{T_e/m_e} \right)$ is the electron thermal velocity. The dust charging rate can be given by $\eta = 0.01\omega_{pe} \frac{n_{e0}}{n_{i0}} \frac{a}{\lambda_D}$. Further, in the absence of beam and dust grain terms i.e., $n_{b0} = 0$, $\delta = 1$, means without dust grains Eq. (13)

gives

$$1 + \frac{\omega_{pe}^2 k_x^2}{\omega_{ce}^2 k^2} - \frac{\omega_{pe}^2 k_z^2}{\omega^2 k^2} - \frac{\omega_{pi}^2 k_x^2}{(\omega^2 - \omega_{ci}^2) k^2} = 0. \quad (14)$$

Considering Eq. (14) and applying conditions essential for TG wave i.e., $\omega_{pi} \ll \omega \ll \omega_{ce}$, we get

$$\omega = (\omega_{pe} k_z) / k_{\perp} \quad \text{as } (\omega_{pe} / \omega_{ce}) \ll 1 \quad [22, 23] \quad (15)$$

where $k = \sqrt{k_{\perp}^2 + k_z^2}$, $k_z \ll k_{\perp}$.

Equation (15) is the standard dispersion relation for TG mode [22, 23] in the infinite geometry.

Equation (13) can further be rewritten as

$$(\omega^2 - \chi_1^2)(\omega^2 - \chi_2^2)(\omega - k_z v_{b0})^2 = \frac{1}{\gamma_0^3} \omega_{pb}^2 \omega^2 (\omega^2 - \omega_{ci}^2) \frac{k_z^2}{k^2}, \quad (16)$$

where

$$\chi_1^2 = \frac{\left(\frac{\omega_{TG}^2 \omega_{ci}^2 k_z^2 m_i}{k^2 m_e} - \frac{i\beta \omega_{TG}^2 \omega_{ci}^2 k_z^2}{(\omega + i\eta)\delta k^2} + \frac{i\beta \omega_{TG}^2 \omega_{ci}^2 m_i k_z^2}{(\omega + i\eta)m_e k^2} - \frac{\omega_{pd}^2 \omega_{ci}^2}{K''} \right)}{\left(\omega_{ci}^2 + \frac{\omega_{TG}^2 m_i k_z^2}{m_e k^2} + \frac{\omega_{TG}^2 k_x^2}{k^2} + \frac{i\beta \omega_{TG}^2 k_x^2}{(\omega + i\eta)k^2} + \frac{i\beta \omega_{TG}^2 k_z^2}{(\omega + i\eta)k^2} \right)}, \quad (17)$$

$$\left(\frac{i\beta \omega_{TG}^2 k_z^2}{(\omega + i\eta)\delta k^2} + \frac{i\beta \omega_{TG}^2 \omega_{ci}^2 m_i k_x^2}{(\omega + i\eta)\omega_{ce}^2 m_e k^2} + \frac{i\beta \omega_{TG}^2 m_i k_z^2}{(\omega + i\eta)m_e k^2} - \frac{\omega_{pd}^2}{K''} \right)$$

where $\omega_{TG}^2 = \omega_{pi}^2 / K''$, $K'' = 1 + \frac{\omega_{pe}^2 k_x^2}{\omega_{ce}^2 k^2}$ and

$$\chi_2^2 = \frac{\omega_{ci}^2}{1 + \frac{k^2 m_e}{k_z^2 m_i}}.$$

In Eq. (16) $\omega \approx \chi_1$ associates with Gould-Trivelpiece mode, $\omega \approx \chi_2$ associates with ion-cyclotron mode and $\omega = k_z v_{b0}$ associates with beam mode. We are looking for the solution when $\chi_1 \approx k_z v_{b0}$ (i.e., when the beam mode is in Cerenkov resonance with the Gould-Trivelpiece mode). Here, the two factors on the LHS of Eq. (16) will become zero simultaneously, when electron beam is not present. From Eq. (16), in the absence of beam ($n_{b0} = 0$) and dust grains i.e. $\delta (= n_{i0} / n_{e0}) = 1$, we recover the expression

$$\omega^2 = \omega_{TG}^2 \left(1 + \frac{m_i k_z^2}{m_e k^2} \right), \quad \omega_{TG}^2 = \omega_{pi}^2 / \left(1 + \frac{\omega_{pe}^2 k_x^2}{\omega_{ce}^2 k^2} \right).$$

Equation (17) can be further rewritten as

$$|\chi_1| = \left[\left(\frac{L_1 L_3 + L_2 L_4}{L_3^2 + L_4^2} \right)^2 + \left(\frac{L_1 L_4 + L_2 L_3}{L_3^2 + L_4^2} \right)^2 \right]^{1/4}, \quad (18)$$

where

$$L_1 = \omega_{ci}^2 \omega_{TG}^2 \frac{k_z^2 m_i}{k^2 m_e} + \frac{\beta \eta \omega_{TG}^2}{(\omega^2 + \eta^2)} \omega_{ci}^2 \frac{k_z^2}{k^2} \left(\frac{1}{\delta} + 1 \right) - \frac{\omega_{pd}^2 \omega_{ci}^2}{K''}, \quad L_2 = \frac{\beta \omega \omega_{TG}^2}{(\omega^2 + \eta^2)} \omega_{ci}^2 \frac{k_z^2}{k^2} \left(\frac{1}{\delta} + 1 \right),$$

$$L_3 = \omega_{ci}^2 + \omega_{TG}^2 \frac{m_i k^2}{m_e k_z^2} - \frac{\omega_{pd}^2}{K''} + \frac{\beta \eta \omega_{TG}^2}{(\omega^2 + \eta^2)} \left(\frac{k_x^2}{k^2} + \frac{k_z^2}{k^2} \frac{1}{\delta} + \frac{m_i \omega_{ci}^2 k_x^2}{m_e \omega_{ce}^2 k^2} + \frac{m_i k_z^2}{m_e k^2} \right),$$

$$L_4 = \frac{\beta\omega\omega_{TG}^2}{(\omega^2 + \eta^2)} \left(\frac{k_x^2}{k^2} + \frac{k_z^2}{k^2} \frac{1}{\delta} + \frac{m_i\omega_{ci}^2}{m_e\omega_{ce}^2} \frac{k_x^2}{k^2} + \frac{m_i}{m_e} \frac{k_z^2}{k^2} \right).$$

When the electron beam exists, we expand the frequency ω as $\omega = \chi_1 + \Lambda_1 = k_z v_{b0} + \Lambda_1$, where Λ_1 is the small frequency discrepancy due to the finite value on RHS of Eq. (16).

Following Mikhailovski [24], the growth rate of the unstable mode is given as

$$\Gamma = \text{Im } \Lambda_1 = \frac{\sqrt{3}}{2} \left[\frac{\omega_{pb}^2 k_z^2 \chi_1 (\chi_1^2 - \omega_{ci}^2)}{2\gamma_0^3 (\chi_1^2 - \chi_2^2) k^2} \right]^{1/3}. \quad (19)$$

If beam voltage is V_b , ω_r is the real part of the frequency associated with instability and $k^2 = k_x^2 + k_z^2$, then

$$\omega_r = k_z \left[2eV_b/m \right]^{1/2} - \frac{1}{2} \left[\frac{\omega_{pb}^2 k_z^2 \chi_1 (\chi_1^2 - \omega_{ci}^2)}{2\gamma_0^3 (\chi_1^2 - \chi_2^2) k^2} \right]^{1/3}, \quad (20)$$

and ω_r increases with the beam voltage similar to the experimental observation of Chang [9] (cf. Figure 4(a) of Chang [9]).

The phase velocity of the unstable mode is

$$v_{ph} = \frac{\omega_r}{k_z} = \left[2eV_b/m \right]^{1/2} - \frac{1}{2k_z} \left[\frac{\omega_{pb}^2 k_z^2 \chi_1 (\chi_1^2 - \omega_{ci}^2)}{2\gamma_0^3 (\chi_1^2 - \chi_2^2) k^2} \right]^{1/3}. \quad (21)$$

From Eq. (21), we can say that the phase velocity of the unstable mode increases with the beam voltage V_b .

2.2 Finite Geometry

Consider a cylinder of radius ' a_1 ' containing uniform plasma with negatively charged dust grains, electrons and ions. The perturbed densities of electron, ion, dust and beam for finite geometry, derived using equations of motion and continuity (cf. Eqs. (2), (3) and (7)) are given as

$$\begin{aligned} n_{1e} &= -\frac{n_{e0}e}{m_e} \left[\frac{-\nabla_{\perp}^2 \Phi}{\omega^2 - \omega_{ce}^2} + \frac{k_z^2 \Phi}{\omega^2} \right], \\ n_{1i} &= \frac{n_{i0}e}{m_i} \left[\frac{-\nabla_{\perp}^2 \Phi}{\omega^2 - \omega_{ci}^2} + \frac{k_z^2 \Phi}{\omega^2} \right], \\ n_{1d} &= \frac{-n_{d0}Q_{d0}k_z^2 \Phi}{m_d \omega^2}, \quad \text{and} \\ n_{1b} &= \frac{-n_{b0}ek_z^2 \Phi}{m_0 \gamma_0^3 (\omega - k_z v_{b0})^2}. \end{aligned}$$

Following the similar instability analysis as was done in infinite geometry, we obtain

$$\begin{aligned} \nabla_{\perp}^2 \left(-\frac{\omega_{pe}^2}{\omega_{ce}^2} + \frac{\omega_{pi}^2}{\omega^2 - \omega_{ci}^2} + \frac{i\beta}{(\omega + i\eta)} \frac{\omega_{pe}^2 m_e}{(\omega^2 - \omega_{ci}^2) m_i} - \frac{i\beta}{(\omega + i\eta)} \frac{\omega_{pe}^2}{\omega_{ce}^2} + \frac{\omega_{pd}^2}{\omega^2} \right) \Phi \\ + \left(-1 + \frac{\omega_{pe}^2}{\omega^2} + \frac{\omega_{pi}^2}{\omega^2} - \frac{i\beta}{(\omega + i\eta)} \frac{\omega_{pe}^2 m_e}{\omega^2 m_i} + \frac{i\beta \omega_{pe}^2}{(\omega + i\eta) \omega^2} + \frac{\omega_{pd}^2}{\omega^2} \right) k_z^2 \Phi = \frac{\omega_{pb}^2 k_z^2 \Phi}{\gamma_0^3 (\omega - k_z v_{b0})^2}. \quad (22) \end{aligned}$$

Rewriting Eq. (22) for axially symmetric case, we obtain

$$\frac{\partial^2 \Phi}{\partial r^2} + \frac{1}{r} \frac{\partial \Phi}{\partial r} + p^2 \Phi = -\frac{\omega_{pb}^2 k_z^2 \Phi}{\gamma_0^3 (\omega - k_z v_{b0})^2 l_2^2}, \quad (23)$$

where

$$p^2 = l_1^2 / l_2^2, \quad (24)$$

$$l_1^2 = \left(-k_z^2 + \frac{\omega_{pe}^2 k_z^2}{\omega^2} + \frac{\omega_{pi}^2 k_z^2}{\omega^2} - \frac{i\beta}{\omega + i\eta} \frac{\omega_{pe}^2 m_e k_z^2}{\omega^2 m_i} + \frac{i\beta \omega_{pe}^2 k_z^2}{(\omega + i\eta)\omega^2} + \frac{\omega_{pd}^2 k_z^2}{\omega^2} \right),$$

$$l_2^2 = \left(-\frac{\omega_{pe}^2}{\omega_{ce}^2} + \frac{\omega_{pi}^2}{\omega^2 - \omega_{ci}^2} + \frac{i\beta}{\omega + i\eta} \frac{\omega_{pe}^2 m_e}{(\omega^2 - \omega_{ci}^2) m_i} - \frac{i\beta}{\omega + i\eta} \frac{\omega_{pe}^2}{\omega_{ce}^2} + \frac{\omega_{pd}^2}{\omega^2} \right).$$

If we neglect the terms containing dust, we can rewrite Eq. (24) as

$$p^2 = \frac{\left(-1 + \frac{\omega_{pe}^2}{\omega^2} + \frac{\omega_{pi}^2}{\omega^2} \right) k_z^2}{\left(-\frac{\omega_{pe}^2}{\omega_{ce}^2} + \frac{\omega_{pi}^2}{\omega^2 - \omega_{ci}^2} \right)}. \quad (25)$$

In case relativistic electron beam is not present, Eq. (23) can be rewritten as

$$\frac{\partial^2 \Phi}{\partial r^2} + \frac{1}{r} \frac{\partial \Phi}{\partial r} + p^2 \Phi = 0. \quad (26)$$

Equation (26) is a well-known Bessel equation hence the solution can be given as $\Phi = LJ_0(p_{l1}t) + MY_0(p_{l1}t)$, where L and M are constants. J_0 represents the 0th order Bessel function of 1st kind whereas Y_0 represents the 0th order Bessel function the 2nd kind.

At $t = 0$, $Y_0 \rightarrow \infty$ and hence $M = 0$, $\Phi = LJ_0(p_{l1}t)$, $p = p_{l1}$. At $t = a_1$, Φ must vanish, hence, $J_0(p_{l1}a_1) = 0$, $p_{l1} = \frac{X_l}{a_1}$, ($l = 1, 2, \dots$), where X_l are the zeros of the Bessel function $J_0(X)$. The electron beam being present in the system, the solution of wave-function Φ can be stated as orthogonal sets of wave-function

$$\Phi = \sum_n A J_0(p_n t). \quad (27)$$

Further, using the value of Φ in Equation (23) from Equation (27) and multiplying both the sides of Eq.(23) by $tJ_0(p_{l1}t)$ and integrating over t from 0 to a_1 , here radius of plasma is a_1 , retaining only the dominant mode $n = l$, we obtain

$$p^2 - p_{l1}^2 = -\frac{\omega_{pb}^2 k_z^2 \beta''}{\gamma_0^3 (\omega - k_z v_{b0})^2 l_2^2}, \quad (28)$$

where

$$\beta'' = \begin{cases} \frac{\int_0^{t_b} t J_0(p_n t) J_0(p_{l1} t) dr}{\int_0^{a_1} t J_0(p_n t) J_0(p_{l1} t) dr} & \text{if } t_b \neq a_1 \\ 1 & \text{if } t_b = a_1. \end{cases}$$

Putting the value of p^2 from Eq. (24), Eq. (28) can be rewritten as

$$(\omega^2 - \alpha_2^2)(\omega - k_z v_{b0})^2 = \frac{\omega_{pb}^2 k_z^2 \omega^2 \beta''}{\gamma_0^3 (p_{l1}^2 + k^2)} \quad (29)$$

where

$$\alpha_2^2 = \frac{h_1^2}{h_2^2}, \quad (30)$$

$$h_1^2 = m_1 + im_2,$$

$$m_1 = \left(\omega_{pe}^2 k_z^2 / (p_{l1}^2 + k_z^2) \right) + \omega_{pd}^2 - \frac{\beta\eta}{(\omega^2 + \eta^2)} \left(k_z^2 / (p_{l1}^2 + k_z^2) \right) \omega_{pe}^2 \left(\frac{m_e}{m_i} - 1 \right),$$

and

$$m_2 = -\frac{\beta\omega}{(\omega^2 + \eta^2)} \left(k_z^2 / (p_{l1}^2 + k_z^2) \right) \omega_{pe}^2 \left(\frac{m_e}{m_i} - 1 \right),$$

$$h_2^2 = m_3 + im_4,$$

$$m_3 = 1 + \frac{p_{l1}^2}{(p_{l1}^2 + k_z^2)} \frac{\omega_{pe}^2}{\omega_{ce}^2} + \frac{p_{n1}^2}{(p_{l1}^2 + k_z^2)} \frac{\omega_{pi}^2}{\omega^2 - \omega_{ci}^2} - \frac{\beta\eta}{(\omega^2 + \eta^2)} \frac{p_{l1}^2}{(p_{l1}^2 + k_z^2)} \left(\frac{\omega_{pe}^2}{\omega^2 - \omega_{ci}^2} + \frac{\omega_{pe}^2}{\omega_{ce}^2} \right),$$

and

$$m_4 = -\frac{\beta\eta}{(\omega^2 + \eta^2)} \frac{p_{l1}^2}{(p_{l1}^2 + k_z^2)} \left(\frac{\omega_{pe}^2}{\omega^2 - \omega_{ci}^2} + \frac{\omega_{pe}^2}{\omega_{ce}^2} \right).$$

Therefore,

$$|\alpha_2| = \left[\left(\frac{m_1 m_3 + m_2 m_4}{m_3^2 + m_4^2} \right)^2 + \left(\frac{m_2 m_3 + m_1 m_4}{m_3^2 + m_4^2} \right)^2 \right]^{1/4}. \quad (31)$$

Considering Eq. (31) and applying condition essential for TG wave ($k_z \ll k_\perp$, $\omega_{pi} \ll \omega \ll \omega_{ce}$, we will get

$$\omega = (\omega_{pe} k_z) / k_\perp \text{ as } (\omega_{pe} / \omega_{ce}) \ll 1 \quad [22, 23],$$

where $k_\perp = \frac{X_l}{a_1}$.

Following the similar process as was done in infinite geometry, the unstable mode's growth rate in finite geometry is given as

$$\Gamma = Im\Lambda_1 = \frac{\sqrt{3}}{2} \left[\frac{\omega_{pb}^2 k_z^2 |\alpha_2| \beta''}{2\gamma_0^3 [(X_l/a_1)^2 + k_z^2] h_2^2} \right]^{1/3}. \quad (32)$$

The real part of unstable mode's frequency is

$$\omega_r = k_z \left(\frac{2eV_b}{m_b} \right)^{1/2} - \frac{1}{2} \left[\frac{\omega_{pb}^2 k_z^2 |\alpha_2| \beta''}{2\gamma_0^3 [(X_l/a_1)^2 + k_z^2] h_2^2} \right]^{1/3}. \quad (33)$$

In this case also the real part of the frequency of unstable mode increases with beam voltage which shows the similarity with the experimental observation of Chang [9].

The phase velocity of the unstable mode is

$$v_{ph} = \frac{\omega_r}{k_z} = \left(\frac{2eV_b}{m_b} \right)^{1/2} - \frac{1}{2k_z} \left[\frac{\omega_{pb}^2 k_z^2 |\alpha_2| \beta''}{2\gamma_0^3 [(X_n/a_1)^2 + k_z^2] h_2^2} \right]^{1/3}. \quad (34)$$

3. Numerical Analysis

In the present calculations, a typical set of dusty plasma parameters are taken into account. The parameters used for calculations are: ion plasma density $n_{i0} = 10^9 \text{ cm}^{-3}$, electron plasma density $n_{e0} = 0.5 \times 10^9 - 0.125 \times 10^9 \text{ cm}^{-3}$, $m_d = 10^{12} m_p$ (for dust grain radius of $1 \mu\text{m}$ density of $\sim 1 \text{ g cm}^{-3}$), temperature of electrons $T_e = 0.22 \text{ eV}$ and temperature of ions = 0.15 eV , radius of plasma cylinder $a_1 = 2 \text{ cm}$, radius of beam $r_b = 1.5 \text{ cm}$, guide magnetic field $B_s = 0.38 \times 10^3 \text{ G}$, number density of dust particles $n_{d0} = 0.8 \times 10^4 \text{ cm}^{-3}$, $m_i/m_e = 7.16 \times 10^4$ for potassium plasma and the average dust grain size $a = 0.6 \mu\text{m}$.

The dispersion curves of TG waves along with REB (*relativistic electron beam*) mode are plotted in Figure 1 for infinite geometry and Figure 2 for finite geometry, using Eqs. (18) (for infinite case) and Eq. (31) (for finite case) for different values of δ ($= 2, 3, 4, 5$). In both the geometries the energy of the beam is taken to be 0.0284 MeV so that the beam must possess relativistic velocity $= 1 \times 10^{10} \text{ cm/sec}$. In Figure 1 and Figure 2, we have chosen the energy of REB such that the TG wave and beam mode intersect with each other at the same frequencies. The points of intersection of beam and TG mode are written in tabular form: Table 1 (infinite case) and Table 2 (finite case) in which the frequencies and the corresponding wave numbers for various values of δ are written. It can be seen that the frequencies of unstable mode increases with wave number (cf. Figure 1 and Figure 2) for all values of δ . At these frequencies the relativistic electron beam interacts with TG wave and transfers its energy to latter, thus the wave becomes unstable and grows which leads to the instability. It is significant to mention here that the TG mode exist when $k_{\perp} = k$, $k_z \ll k_{\perp}$. From Table 1 and Table 2 it can be seen that the unstable modes' frequency increases with the increase in δ for both the cases. As the value of δ rises, the electron density of plasma n_{e0} falls. As the value of δ increases i.e., the proportion of the negative charge per unit volume inherent by the dust particles becomes more, as a consequent, the unstable mode frequency enhances, which in turn decreases the wave damping.

Table 1. From Figure 1 (electron beam and plasma containing negatively charged dust particles) we acquire the values of frequencies of unstable mode and axial wave number k_z (cm^{-1}) for diverse values of δ for infinite geometry.

$\delta (= n_{i0}/n_{e0})$	ω (rad/sec) $\times 10^7$	k_z (cm^{-1})
2	0.223	0.003
3	0.271	0.004
4	0.326	0.0045
5	0.432	0.0054

Table 2. From Figure 2 (electron beam and plasma containing negatively charged particles) we acquire the values of frequencies of unstable mode and axial wave number k_z (cm^{-1}) for diverse values of δ for finite geometry.

$\delta (= n_{i0}/n_{e0})$	ω (rad/sec) $\times 10^5$	k_z (cm^{-1})
2	0.00119	0.0011
3	0.00129	0.0015
4	0.00142	0.0020
5	0.00275	0.0031

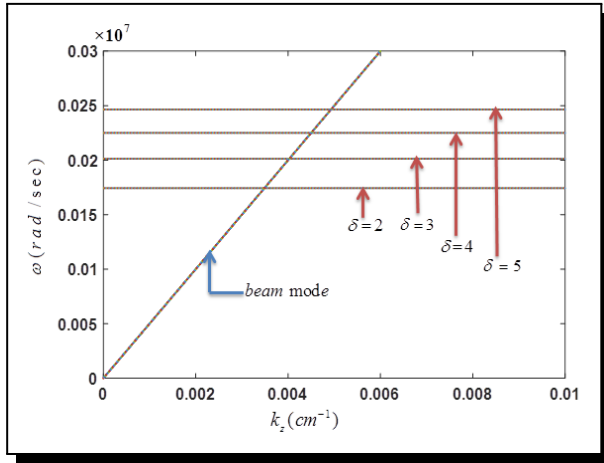


Figure 1. Dispersion curves of TG mode over a plasma containing negatively charged particles for $\delta = 2, 3, 4, 5$ and a beam mode for infinite geometry. The parameters are mentioned in the text.

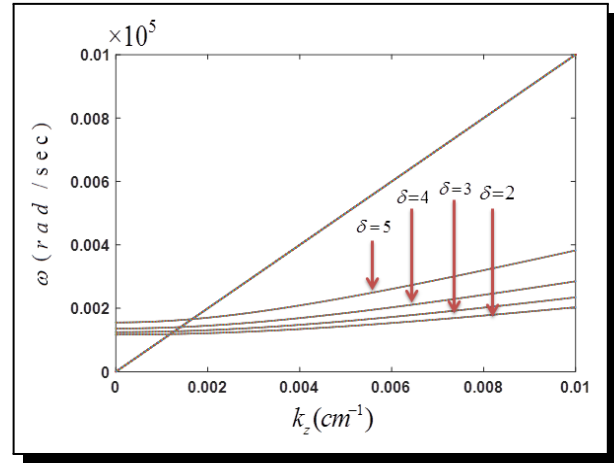


Figure 2. Dispersion curves of TG mode over a plasma containing negatively charged particles for $\delta = 2, 3, 4, 5$ and a beam mode for finite geometry. The parameters are mentioned in the text.

Again, considering the dust charge fluctuations effect appreciably small (by considering small values of dust grains' size and dust grain density n_{d0}) using Eq. (19) for infinite geometry and Eq. (32) for finite geometry and taking the values of ϑ (rad/sec) from the respective tables of infinite and finite geometry, the unstable wave's growth rate Γ (sec^{-1}) as a function of δ taking different values of beam density say $n_{b0} = 4 \times 10^9 \text{ cm}^{-3}$, $5 \times 10^9 \text{ cm}^{-3}$ and $1 \times 10^{10} \text{ cm}^{-3}$, are plotted, keeping all other parameters constant. In Figure 3 for infinite geometry and Figure 4 for finite geometry, it can be shown that the growth rate at which the instability grows enhanced as the density of relativistic electron beam rises for all the values of δ . This happens because the dust particles in plasma have tendency to stick the electrons and as the density of beam electrons increases more and more electrons will be captured by the dust grains through the beam in dusty plasma. Hence the critical drift for the excitation of wave decreases and hence the growth rate increases. For $\delta = 1$ i.e., without dust grains, the value of the growth rate $\Gamma = 0.021 \times 10^6 \text{ sec}^{-1}$ for infinite geometry and $\Gamma = 0.0011 \times 10^4 \text{ sec}^{-1}$ for finite geometry. It can also be seen from Figure 3 and Figure 4 that the unstable mode's growth rate enhanced with the beam density and varies as the cube root of beam density (cf. Eqs. (19) and (32)) in both the geometries. From Eq. (20) for infinite geometry and Eq. (33) for finite geometry we can see that the unstable mode's real frequency varies as square root of the beam voltage. Our results are similar with the experimental findings of Chang [9] without dust grains case. Also, Eq. (21) and Eq. (34) show that the phase velocity of the TG mode increases with the beam energy for both the geometries. Moreover, on comparing the growth rate of infinite geometry (cf. Figure 3) and for finite geometry (cf. Figure 4), we have found that the growth rate is

more in case of infinite geometry. This is due to non-local effects because the interaction region decreases in case of finite geometry. Also, Equation (32) indicates that as the radius of cylindrical waveguide (a_1) decreases the growth rate will also decrease as it is inversely proportional to $k[k^2 = (\bar{X}_n/a_1)^2 + k_z^2]$ in case of finite geometry.

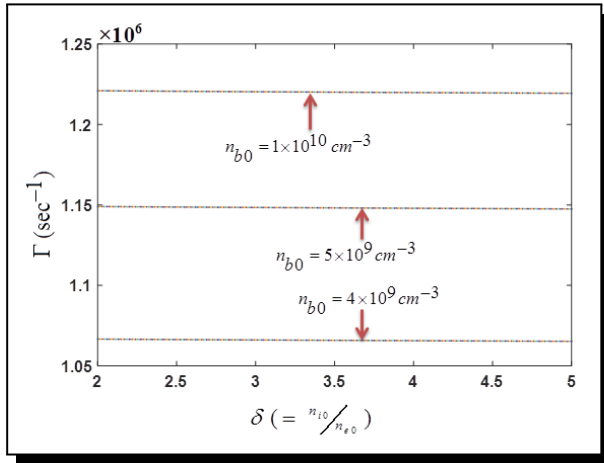


Figure 3. Growth rate of the unstable TG mode Γ (sec^{-1}) vs. $\delta (= n_{i0}/n_{e0})$ for the similar parameters as in Figure 1 for three different values of beam density, say, $n_{b0} = 4 \times 10^6 \text{ cm}^{-3}$, $6 \times 10^6 \text{ cm}^{-3}$ and $8 \times 10^6 \text{ cm}^{-3}$ for infinite geometry.

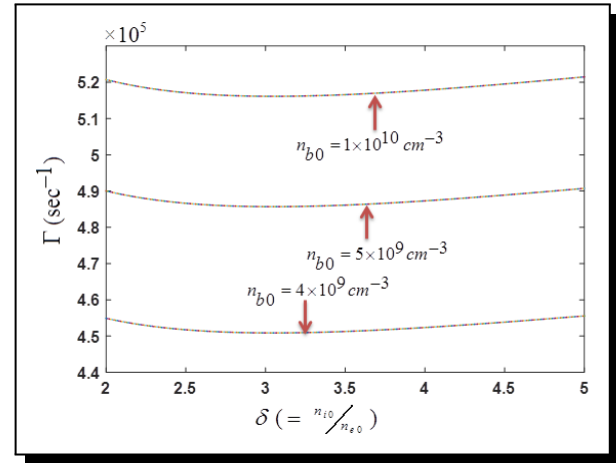


Figure 4. Growth rate of the unstable TG mode Γ (sec^{-1}) vs. $\delta (= n_{i0}/n_{e0})$ for the similar parameters as in Figure 2 and for three different values of beam density, say, $n_{b0} = 4 \times 10^6 \text{ cm}^{-3}$, $6 \times 10^6 \text{ cm}^{-3}$ and $8 \times 10^6 \text{ cm}^{-3}$ for finite geometry.

Using Eq. (18) for infinite geometry and Eq. (31) for finite geometry, we have plotted the frequencies of unstable mode with respect to the size of the dust grains ' a ' for various values of δ say 2, 3, 4, 5 keeping all other parameters constant. Figure 5 for infinite and Figure 6 for finite geometry display the variation of frequency of unstable wave with respect to the size of the dust grains ' a ' for different values of δ . It is observed that the frequencies of unstable mode decrease with increase in the dust grains' size in both the geometries. Again, using Eq. (19) for infinite and Eq. (32) for finite geometry we have plotted the growth rate Γ (sec^{-1}) against dust grains' size ' a ' for different values of δ keeping all other parameters constant. Figure 7 for infinite case and Figure 8 for finite case show the deviation of growth rate with respect to the size of dust grains ' a ' for different values of δ . It is found that the growth rate decreases with dust grains' size ' a '. It is because when the radii of the dust grains increases, the number of electrons sticking to the dust grains also increases. As the number of electrons grabbed by the dust grains increases the dust grain surface potential starts to decline which in turn drops the average dust grain charge Q_{d0} . As the average dust grain charge Q_{d0} drops, the dust grains try to compensate it by taking more and more electrons from ambient plasma, therefore the frequencies of TG wave decreases, hence the enhancement rate of instability also falls with increase in dust grain size for all the values of δ .

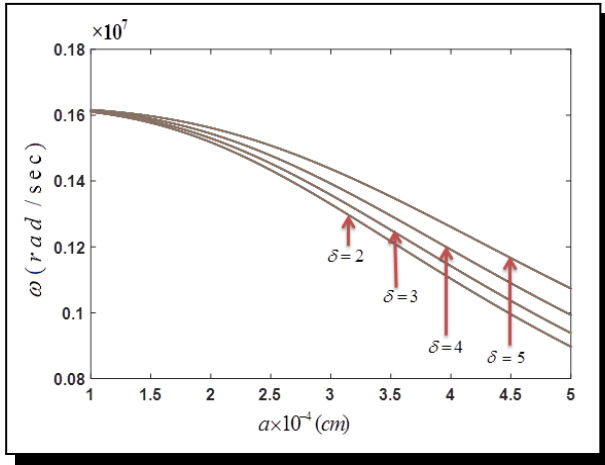


Figure 5. Unstable TG wave’s frequencies ω (rad/sec) vs. dust grains size ‘a’ for infinite geometry.

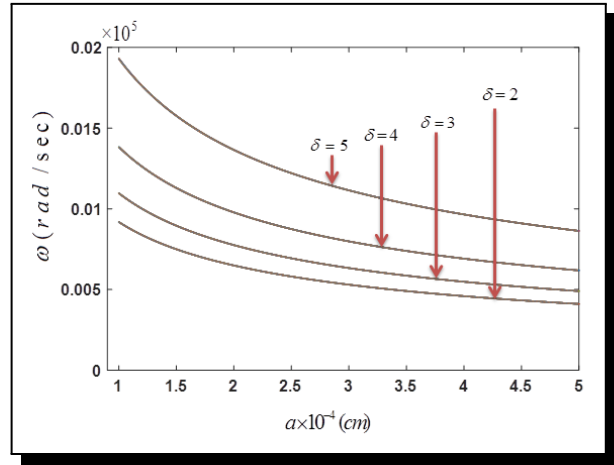


Figure 6. Unstable TG wave’s frequencies ω (rad/sec) vs. dust grains size ‘a’ for finite geometry.

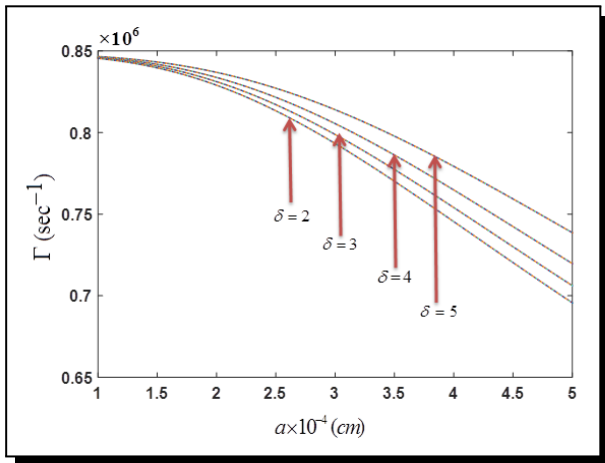


Figure 7. Growth rate of the unstable TG wave Γ (sec^{-1}) vs. dust grains size ‘a’ for infinite geometry.

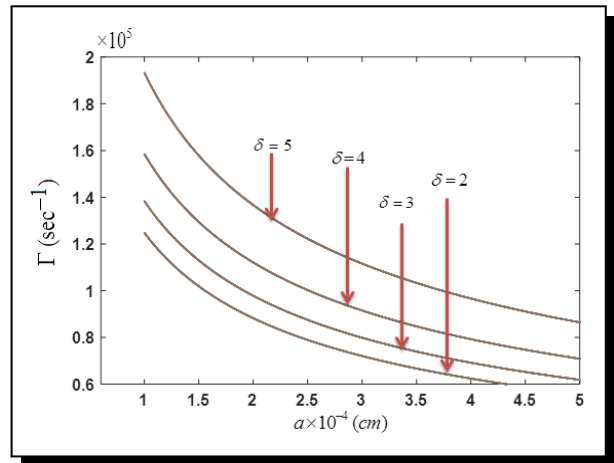


Figure 8. Growth rate of the unstable TG wave Γ (sec^{-1}) vs. dust grains size ‘a’ for finite geometry.

Moreover, using Eq. (18) for infinite geometry and Eq. (31) for finite geometry we have plotted the frequencies of unstable mode with respect to the number density of dust grain ‘ n_{d0} ’ for different values of δ , keeping all other parameters constant. Figure 9 for infinite and Figure 10 for finite geometry display the variation of frequencies of unstable wave with respect to the dust grain density ‘ n_{d0} ’ for mentioned values of δ . It is observed that the frequencies of unstable mode decrease with the increase in dust grain number density ‘ n_{d0} ’ in both the geometries. Again, using Eqs. (19) and (32) of infinite and finite geometry respectively, the growth rate Γ (sec^{-1}) as a function of dust grain number density ‘ n_{d0} ’ are plotted, considering other parameters as constant. Figure 11 for infinite and Figure 12 for finite geometry show the variation of growth rate of instability with respect to dust grain number density ‘ n_{d0} ’ for

different values of δ . It is found that the growth rate of unstable mode Γ (sec^{-1}) decreases with increase in dust grain number density ' n_{d0} '. This happens because when the number density of dust grains increases need of electrons for dust grains also increases, as we know that the dust grains have temptation to electrons. The number density of dust particles increase and the number of electrons available per dust particles decreases which lessens Q_{d0} (the average dust grain charge), hence the frequency and the growth rate of the instability associated with TG wave also decreases. Our findings show similarity with the theoretical observations of Tribeche et al. [27].

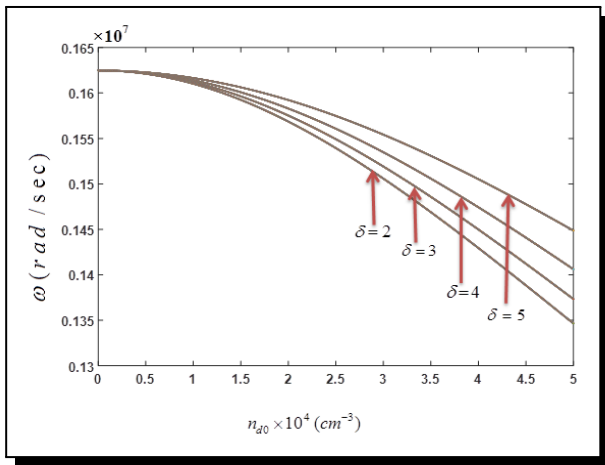


Figure 9. Unstable TG wave's frequencies ω (rad/sec) vs. number density of dust grains ' n_{d0} ' for infinite geometry.

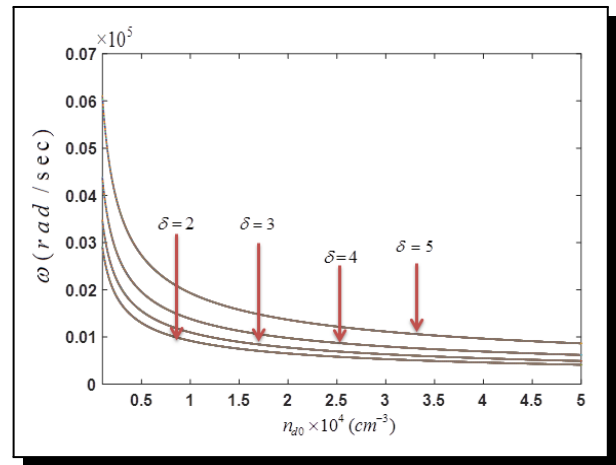


Figure 10. Unstable TG wave's frequencies ω (rad/sec) vs. number density of dust grains ' n_{d0} ' for finite geometry.

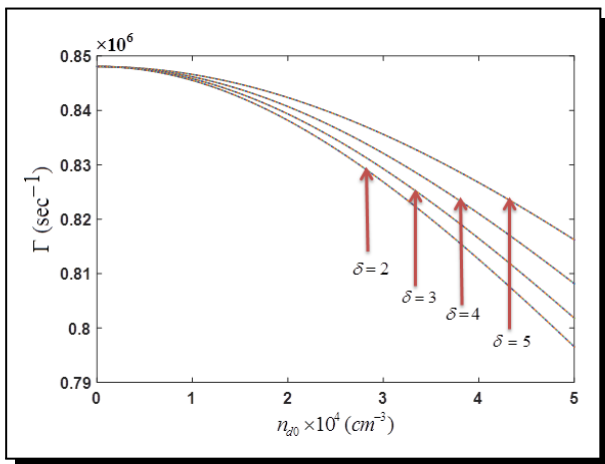


Figure 11. Growth rate of the unstable TG mode Γ (sec^{-1}) vs. number density of dust grains ' n_{d0} ' for infinite geometry.

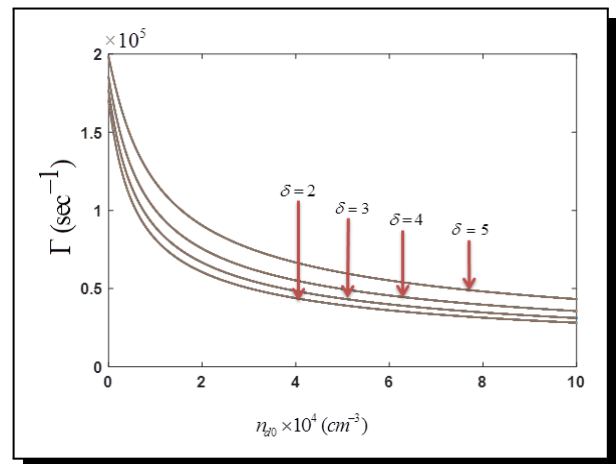


Figure 12. Growth rate of the unstable TG mode Γ (sec^{-1}) vs. number density of dust grains ' n_{d0} ' for finite geometry.

Again, using Eqs. (19) and (32) for infinite and finite geometry respectively, the growth rate Γ (sec^{-1}) as a function of relativistic gamma factor γ_0 for different values of δ are plotted. It is

found that the growth rate decreases with increase in the values of relativistic gamma factor for infinite (cf. Figure 13) as well as for finite geometry (cf. Figure 14). It is attributed to the fact, the phase velocity of Gould-Trivelpiece wave does not match with the beam velocity as the relativistic gamma factor increases and hence the growth rate decreases.

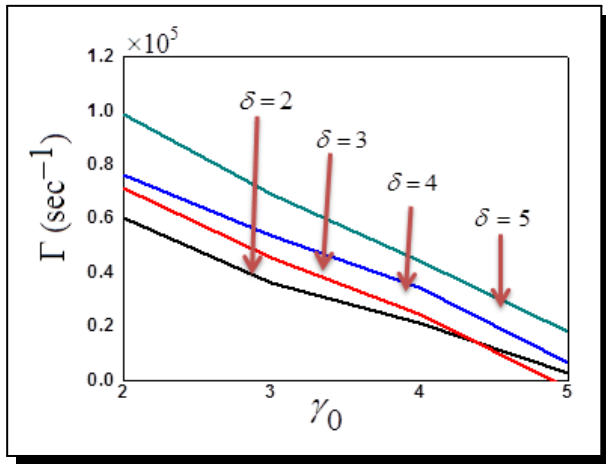


Figure 13. Growth rate of the unstable TG mode Γ (sec^{-1}) vs. relativistic gamma factor γ_0 for infinite geometry.

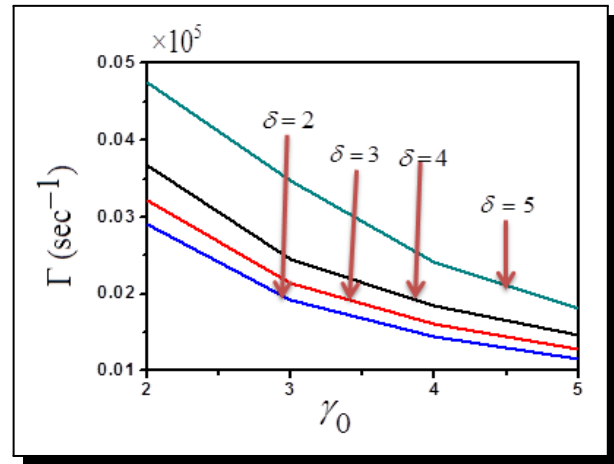


Figure 14. Growth rate of the unstable TG mode Γ (sec^{-1}) vs. relativistic gamma factor γ_0 for finite geometry.

4. Conclusion

The excitation of Gould-Trivelpiece mode by a REB has been studied in dusty plasma as well as in dusty plasma cylinder. The instability arises due to the interaction of REB with dusty plasma species through Cerenkov interaction. The frequency and the growth rate of the unstable TG mode upraise with an increase in relative density of negatively charged dust grains δ . It is also observed that the growth rate is more in case of infinite geometry as compared to that of finite geometry due to decline in the interaction region. It is also found that the growth rate enhances with an increase in number density of electrons possess by beam, in both the geometries and varies as the cube root of the beam density. This result shows resemblance with the experimental observations of Chang [9] without dust grains. Our growth rate results with negatively charged dust grains show qualitativesimilarity with the experimental observations of Barkan *et al.* [25], and theoretical predictions of Chow and Rosenberg [26] and Tribeche *et al.* [27]. Thus, the instability of Gould-Trivelpiece mode destabilizes in the presence of negatively charged dust grains in this model. Presence of relativistic electron beam excites Gould-Trivelpiece mode and its growth rate expressively depends on beam density, dust grain size and number density of dust particles, and relativistic gamma factor. This work may advantageous in plasma processing of material experiments [28] because dust appeared to be key source of contamination during material manufacturing and in enhanced backscatter from the Space Shuttle exhaust [29].

Acknowledgements

One of the authors (D. Kaur) is thankful to Dr. Ruby Gupta (Department of Physics, Swami Shraddhanand College, University of Delhi) for fruitful discussions.

Competing Interests

The authors declare that they have no competing interests.

Authors' Contributions

All the authors contributed significantly in writing this article. The authors read and approved the final manuscript.

References

- [1] A.W. Trivelpiece and R.W. Gould, Space charge waves in cylindrical plasma columns, *Jour. Appl. Phys.* **30** (1959), 1784.
- [2] J.H. Malmberg and C.B. Wharton, Dispersion of electron plasma waves, *Phys. Rev. Lett.* **17** (1966), 175.
- [3] W.M. Mannheimer, Nonlinear development of an electron plasma wave in a cylindrical waveguide, *Phys. Fluids* **12** (1969), 2426.
- [4] J.P. Lynov, P. Michelsen, H.L. Pecseli, J. Juul Rasmussen, K. Saeki and V.A. Turikov, Observations of solitary structures in a magnetized, plasma loaded waveguide, *Phys. Scr.* **20** (1979), 328.
- [5] H. Schamel, Theory of electron holes, *Phys. Scr.* **20** (1979), 336.
- [6] R.L. Stenzel and J.M. Urrutia, Trivelpiece-Gould modes in a uniform unbounded plasma, *Phys. Plasmas* **23** (2016), 092103.
- [7] G. Praburam and A.K. Sharma, Second-harmonic excitation of a Gould-Trivelpiece mode in a beam-plasma system, *J. Plasma Phys.* **48** (1992), 3.
- [8] S. Seiler, M. Yamada and H. Ikezi, Lower hybrid instability driven by a spiraling ion beam, *Phys. Rev. Lett.* **37** (1976), 700.
- [9] R.P.H. Chang, Lower-hybrid beam-plasma instability, *Phys. Rev. Lett.* **35** (1975), 28.
- [10] S.C. Sharma, M.P. Srivastava, M. Sugawa and V.K. Tripathi, Excitation of lower hybrid waves by a density-modulated electron beam in a plasma cylinder, *Phys. Plasmas* **5** (1998), 3161.
- [11] V. Prakash, R. Gupta, S.C. Sharma and Vijayshri, Excitation of lower hybrid waves by an ion beam in a magnetized plasma, *Laser and Particle Beams* **31** (2013), 747.
- [12] J.B. Pieper and J. Goree, Dispersion of plasma dust acoustic waves in the strong coupling regime, *Phys. Rev. Lett.* **77** (1996), 3137.
- [13] C. Thompson, A. Barkan, N. D'Angelo and R.L. Merlino, Dust acoustic waves in a direct current glow discharge, *Phys. Plasmas* **4** (1997), 2331.
- [14] S.C. Sharma, K. Sharma and R. Walia, Ion beam driven ion-acoustic waves in a plasma cylinder with negatively charged dust grains, *Phys. Plasmas* **19** (2012), 073706.
- [15] S.C. Sharma, D. Kaur, A. Gahlot and J. Sharma, Excitation of dust acoustic waves by an ion beam in a plasma cylinder with negatively charged dust grains, *Phys. Plasmas* **21** (2014), 103702.

- [16] A. Barkan, N. D'Angelo and R.L. Merlino, Experiments on ion-acoustic waves in dusty plasmas, *Planet. Space Sci.* **44** (1996), 239.
- [17] M. Rosenberg, Ion-and dust-acoustic instabilities in dusty plasma, *Planet. Space Sci.* **41** (1993), 229.
- [18] C.S. Liu and V.K. Tripathi, *Introduction of Electromagnetic Waves With Electron Beams and Plasmas*, World Scientific, Singapore (1994).
- [19] E.C. Whipple, T.G. Northrop and D.A. Mendis, The electrostatics of dusty plasma, *J. Geophys. Res.* **90** (1985), 7405.
- [20] M.R. Jana, A. Sen and P.K. Kaw, Collective effects due to charge fluctuation dynamics in a dusty plasma, *Phys. Rev. E* **48** (1993), 3930.
- [21] V. Prakash and S.C. Sharma, Excitation of surface plasma waves by an electron beam in a magnetized dusty plasma, *Phys. Plasmas* **16** (2009), 093703.
- [22] V.K. Jain and P. Khristiansen, Excitation of electron cyclotron harmonic instabilities in a thin beam-plasma system, *J. Plasma Phys. and Contr. Fusion* **26** (1984), 613.
- [23] V.K. Jain and P. Khristiansen, Recurrence of electron cyclotron harmonic wave instability in a beam-plasma system, *J. Plasma Phys. and Contr. Fusion* **25** (1983), 1169.
- [24] A.B. Mikhailovski, *Theory of Plasma Instabilities, Vol. 1, Instabilities of a Homogeneous Plasma*, New York Consultant Burea (1974).
- [25] A. Barkan, N.D'Angelo and R.L. Merlino, Laboratory experiments on electrostatic ion cyclotron waves in a dusty plasma, *Planet. Space Sci.* **43** (1995), 905.
- [26] V.W. Chow and M. Rosenberg, Electrostatic ion cyclotron instability in dusty plasmas, *Planet. Space Sci.* **43** (1995), 613.
- [27] M. Tribeche and T.H. Zerguini, Current-driven dust ion-acoustic instability in a collisional dusty plasma with charge fluctuations, *Phys. Plasmas* **41** (2001), 394.
- [28] K. Ostrikov, U. Cvelbar and A.B. Murphy, Plasma nanoscience: setting directions, tackling grand challenge, *J. Phys. Appl. D: Phys.* **44** (2011), 174001.
- [29] P.A. Bernhardt, G. Ganguli, M.C. Kelley and W.E. Swartz, Enhanced radar backscatter from space shuttle exhaust in the ionosphere, *J. Geophys. Res.* **100** (1995), 23811.